

# Defect-induced ferromagnetism in a $S=1/2$ quasi-one-dimensional Heisenberg antiferromagnetic chain compound

**Zhe Wang**

High Magnetic Field Laboratory, Chinese Academy of Sciences

**Lin Hu**

High Magnetic Field Laboratory, Chinese Academy of Sciences

**Langsheng Lin**

High Magnetic Field Laboratory, Chinese Academy of Sciences

**Yuyan Han**

High Magnetic Field Laboratory, Chinese Academy of Sciences

**Ning Hao**

High Magnetic Field Laboratory, Chinese Academy of Sciences

**Jingtao Xu**

Ningbo Ruiling Advanced Energy Materials Institute Co., Ltd

**Qianwang Chen**

University of Science and Technology of China

**Zhe Qu** (✉ [zhequ@hmfl.ac.cn](mailto:zhequ@hmfl.ac.cn))

High Magnetic Field Laboratory, Chinese Academy of Sciences

---

## Research Article

**Keywords:** ferromagnetism, Heisenberg antiferromagnetic chain (HAFC), magnetic materials

**Posted Date:** February 23rd, 2021

**DOI:** <https://doi.org/10.21203/rs.3.rs-227785/v1>

**License:**   This work is licensed under a Creative Commons Attribution 4.0 International License.

[Read Full License](#)

---

**Version of Record:** A version of this preprint was published at Scientific Reports on July 14th, 2021. See the published version at <https://doi.org/10.1038/s41598-021-93930-1>.

# **Defect-induced ferromagnetism in a $S=1/2$ quasi-one-dimensional Heisenberg antiferromagnetic chain compound**

Zhe Wang,<sup>1,2</sup> Lin Hu,<sup>1,3</sup> Langsheng Lin<sup>1</sup>, Yuyan Han<sup>1</sup>, Ning Hao,<sup>1</sup> Jingtao Xu,<sup>4</sup>  
Qianwang Chen,<sup>1,5</sup> and Zhe Qu<sup>1,3</sup>

*1. Anhui Key Laboratory of Condensed Matter Physics at Extreme Conditions, High Magnetic Field Laboratory, Hefei Institutes of Physical Sciences, Chinese Academy of Sciences, Hefei, Anhui 230031, China.*

*2. Science Island Branch of Graduate School, University of Science and Technology of China, Hefei, Anhui 230026, China.*

*3. CAS Key Lab of Photovoltaic and Energy Conservation Materials, Hefei Institutes of Physical Sciences, Chinese Academy of Sciences, Hefei, Anhui 230031, China.*

*4. Ningbo Ruiling Advanced Energy Materials Institute Co., Ltd, Ningbo, Zhejiang 315500, China*

*5. Hefei National Laboratory for Physical Sciences at Microscale, Department of Materials Science & Engineering, University of Science and Technology of China, Hefei, 230026, Anhui, China*

## **Corresponding author**

Correspondence and requests for materials should be addressed to L. H.

(email: [hulin@hmf.ac.cn](mailto:hulin@hmf.ac.cn)) or Z. Q. (email: [zhequ@hmf.ac.cn](mailto:zhequ@hmf.ac.cn)).

## Abstract

We present evidences that defects in the spin  $S=1/2$  Heisenberg antiferromagnetic chain (HAFC) compound can lead to ferromagnetism by studying the magnetic and thermal properties of the newly discovered quasi-one-dimensional (1D) metal-organic framework  $[\text{CH}_3\text{NH}_3][\text{Cu}(\text{HCOO})_3]$  (MACuF). Our findings suggest that the long-range ferromagnetic order at 3.7 K can be attributed to  $\text{Cu}^{2+}$  ions from the 2D networks constructed by the endpoints of the broken chains. It is worth mentioning that the ferromagnetic saturation field is less than 5 Oe. In such a case, the intrinsic magnetism can emerge in this quasi-1D Heisenberg chain system at the background of the anti-ferromagnetism. This unusual ferromagnetism found in HAFC not only enriches magnetic features in the low-dimensional systems, but helps to understand some of the exotic magnetic phenomena in other real quasi-1D magnetic materials.

## I. Introduction

Mermin–Wagner theorem [1] indicates that no magnetic long range order survives due to the strong spin fluctuations until  $T=0$  in one-dimensional (1D) and two-dimensional (2D) spin systems, regardless of the strength of the exchange interactions between the neighbour spins. However, the real physical materials are three-dimensional by nature. In particular, the quasi-1D magnetic systems, where the magnetic interactions proceed predominantly along one direction, provide the platform to verify the predications from the Mermin–Wagner theorem and to probe the new properties beyond the theorem. For example, many exotic magnetic phenomena, such as Luttinger liquid state [2, 3], continuous incommensurate magnetic phases [4], topological quantum phase transition [5], were experimentally claimed in the quasi-1D Ising chain compounds.

Metal-organic framework (MOF) is a kind of crystal network formed by connecting metal ions with organic ligands, which has received much attention in recent years due to its novel optical, magnetic and dielectric properties [6]. More importantly, MOF possesses great advantages in the construction of low-dimensional magnetic materials because of the larger size of organic ligands that can separate magnetic elements into chains or plains efficiently. Among various formate group MOFs,  $[\text{CH}_3\text{NH}_3][\text{Cu}(\text{HCOO})_3]$  (MACuF) displays a distorted perovskite-like

structure, and has orthorhombic symmetry of space group  $Pnma$  with  $a=8.4573$  Å,  $b=11.4362$  Å,  $c=8.1022$  Å and  $Z=4$  [7]. The structure of MACuF is shown in Fig. 1. The  $\text{Cu}^{2+}$  ion connects its six nearest  $\text{HCOO}^-$  anions and forms a Cu-O octahedron structure. Due to a strong John-Teller effect, the Cu-O octahedron is strongly distorted, four Cu-O bonds are compressed and the other two Cu-O bonds are elongated, which mainly account for the low-dimensional magnetism in this material. The adjacent octahedrons are not coplanar or co-edge, but isolated. Therefore, the magnetic chain formed by this structure is more likely to be strongly isotropic Heisenberg chain.

In this work, we carry out the detailed measurements on magnetic properties and specific heat of MACuF single crystal. The experimental and fitting results prove that this compound is indeed an  $S=1/2$  uniform HAFC system. What's surprising is that the magnetic phase transition at about 3.7 K is related to a ferromagnetic ordered state. Moreover, the ferromagnetic saturation magnetic moment is almost proportional to the paramagnetic defects concentration. We suggest that this ferromagnetism in HAFC is attributed to the long-range ferromagnetic order formed by the  $\text{Cu}^{2+}$  ions in the 2D networks which is formed by chains' defect points.

## II. Results and Discussions

Figure 2 presents the temperature dependence of the static magnetic susceptibility  $\chi=M/H$  for both  $H$  parallel and vertical to  $b$  axis at 200 Oe.

A broad maximum around 46 K displays the one dimensional magnetic nature and indicates a short-range antiferromagnetic exchange interaction [8]. As the temperature decreases, a sudden upturn below 5 K was observed. The susceptibility in both directions is almost identical above 4 K, but the value of susceptibility for  $H$  perpendicular to  $b$  axis is almost twenty times than that of  $H$  parallel to  $b$  axis at 2 K, which is unusual for an antiferromagnet. From previous studies [9], the spin canting is proposed from the spectral analysis. Such specific magnetic moments configurations can account for the measured strong anisotropic susceptibility.

It is well known that the Bonner–Fisher model [8] can describe the  $S=1/2$  uniform HAFC. There is a good initial test of whether a particular compound might be an  $S=1/2$  uniform HAFC through  $\chi^{\max} \cdot T^{\max} = 0.09416 \frac{Ng^2\mu_B^2}{k_B}$  [10], where  $N$  is Avogadro's number,  $g$  is the spectroscopic splitting factor ( $g$ -factor),  $\mu_B$  is the Bohr magneton,  $k_B$  is Boltzmann's constant. For MACuF, we have  $T^{\max}=46.6$  K and  $\chi^{\max}=0.00345$  emu/mol·Oe, respectively. Taking  $g_0=2.096$  from the ESR measurement at 20 K (shown as the inset of Fig. 2), we get  $\chi^{\max} \cdot T^{\max} = 0.09759 \frac{Ng^2\mu_B^2}{k_B}$ . This indicates that MACuF is probably to be a uniform HAFC compound.

Generally, there is a tiny amount of paramagnetic impurities or defects in the quasi-1D materials, resulting in a Curie-Weiss term [11, 12]. For

example, it is found that there is  $\sim 2.8\%$  of the defects of  $\text{Cu}^{2+}$  ions in  $\text{BaCu}_2\text{V}_2\text{O}_8$ , contributing to the Curie tail in the susceptibility [13]. Accordingly, we fitted the susceptibility data above 4 K with the equations including a temperature independent contribution, a Curie-Weiss paramagnetic term and a term from the  $S=1/2$  uniform HAFC. Here, we assume that the weight of the contribution from paramagnetic term is  $p$ . So we have:

$$\chi(T) = \chi_0 + p \cdot \frac{C}{(T - \theta)} + (1 - p) \cdot \chi_{\text{chain}}(T) \quad (1)$$

$$\chi_{\text{chain}}(T) = \frac{Ng^2u_{\text{B}}^2}{k_{\text{B}}T} \frac{0.25+0.14995x+0.30094x^2}{1+1.9862x+0.68854x^2+6.0626x^3} \quad (2)$$

Here,  $\chi_{\text{chain}}(T)$  is the Bonner-Fisher curve [14] with  $x \equiv J/(2k_{\text{B}}T)$ ,  $C$  is the Curie constant, and  $\theta$  is the impurity Weiss temperature. The fitted parameters are  $\chi_0 = 3.937(4) \times 10^{-5}$  emu/mol·Oe,  $p = 1.12 \times 10^{-2}$ ,  $C = 0.208$  emu·K/mol·Oe,  $\theta = 3.796(7)$  K,  $g = 2.108(8)$ ,  $J/k_{\text{B}} = 72.2(1)$  K. It is noted the obtained  $g$  is very close to the value from the ESR measurement (2.096), which indicates the fitting is reasonable. The fitting results are shown in Fig. 2. The results indicate that MACuF is an ideal  $S=1/2$  HAFC system. However, in comparison with  $\text{BaCu}_2\text{V}_2\text{O}_8$ , the situation is remarkably different in quite low temperature regime, where a ferromagnetic order seems to emerge upon further cooling. Such ferromagnetic order is apparently supported by the saturation of the susceptibility when the temperature approaches zero at both two direction, as shown in Fig. 2.

To further prove the emergence of a true ferromagnetic order, we plot several isothermal  $M$  versus  $H$  curves for  $H \perp b$  in Fig. 3. One can find that  $M$ - $H$  curves show the hysteresis loop structure when temperature is below 4 K, and the hysteresis loop disappears for  $T=4$  K. This is a strong evidence to support the ferromagnetic order below 4 K. More interestingly, it is noted that the maximum saturated magnetic moment in the ordered state is  $0.0111 \mu_B/\text{f.u.}$  from Fig. 3. Comparing with the saturation moment of  $\text{Cu}^{2+}$ , the ratio is  $m=M_S/M_{\text{Cu}^{2+}}=1.06\%$ , which is surprisingly close to the fitted paramagnetic defects concentration ( $p=1.12\%$ ) in Eq. (1). In order to further confirm this uncommon result, several different samples were treated by the same process. Their paramagnetic ratio ( $p$ ) obtained by fitting Eq. (1) was basically in agreement with  $m$  as plotted in the top inset of Fig.3. This proves that the ferromagnetism in MACuF is related to defects but unlikely to be originated from canted antiferromagnetic order or other aspects. The bottom inset of Fig.3 depicts the magnetization  $M$  versus  $H$  measured at 2 K. For  $H // b$ ,  $M$  gradually increases from zero and increases linearly after 0.7T. For  $H \perp b$ , a hysteresis loop is observed with the saturation magnetic field of 5 Oe and the saturation magnetic moment of  $M_S=0.0111 \mu_B/\text{f.u.}$  as shown by the main plotting in Fig. 3. After deducting the constant term and the contribution of HAFC,  $M$  increases at the same rate as for  $H // b$  after 0.7 T. This is similar with the magnetization of hard and

easy axis of a ferromagnet. The different behaviors of  $M-H$  at 2 K for two different directions are consistent with the strong anisotropic susceptibilities shown in Fig. 1, and can be also understood by the spin canting effect. The long-range ferromagnetic phase transition at 4 K is settled down by the specific heat measurement, as shown in Fig. 4. There is a  $\lambda$ -like peak in the specific heat curve, and the anomalous peak moves toward high temperature as external magnetic field increases. These are the typical behaviors of ferromagnetic phase transition under magnetic fields.

It is easy to understand that some broken chains, including some surface of the crystal, will inevitably appear during the growth of quasi-1D chain crystals. These broken chains may exist in the form of isolated point defects or localized surface defects inside the crystal. The magnetic moments exist as surface defects could be considered as independent systems and can form long-range ordered state. For MACuF single crystal, it is reasonable to believe that the long-range ferromagnetic order observed at 4 K attributes to the  $\text{Cu}^{2+}$  ions from localized surface defects in the 2D plane, *i.e.*, the  $ac$  plane, as shown in Fig. 1(b). This situation is similar to the ferromagnetism observed in Teflon tape [15]. When a Teflon tape is cut or stretched, there will be many carbon dangling bonds, and each of them carries a magnetic moment of  $1 \mu_{\text{B}}$ . The moments could show ferromagnetic coupling when carbon dangling

bonds formed a 2D network [15].

Such an unexpected long-range ferromagnetic order observed in MACuF is distinctly different from many other HAFC materials, where the interchain coupling usually results in the long-range antiferromagnetic order with very different ordering temperature [16-26]. Here, we provide the solid evidence to prove the long-range ferromagnetic order can be attributed to the  $\text{Cu}^{2+}$  endpoint of the chains, highlighting the important role of the broken chains. Our studies provide a valuable view to help to understand the phase transitions in HAFCs.

### **III. Conclusion**

The magnetic susceptibility and specific heat data of single-crystal MACuF have been measured. The susceptibility above 4 K was decomposed using a Curie-weiss paramagnetic term and the  $S=1/2$  uniform 1D HAFC model. Combining with specific heat results under magnetic fields, we prove the magnetic phase transition at 4 K to the formation of long-range ferromagnetic order arising from  $\text{Cu}^{2+}$  in the 2D plane constructed by endpoints of the chains.

### **IV. Method**

Single crystals of MACuF with dimensions up to  $3\times 3\times 0.5$  mm<sup>3</sup> were prepared by solvothermal method following as reported [7]. Static

magnetic properties were measured with a Quantum Design MPMS-3 superconducting quantum interference device magnetometer between 2 and 300 K in an applied field up to 7 T. The ESR measurements were performed in a Bruker EMXplus10/12 CW spectrometer at X-band frequencies equipped with a continuous He-gas flow cryostat (Oxford Instruments) working in the temperature range  $1.8 \leq T \leq 300$  K. Specific heat was measured by a pulse relaxation method using a commercial calorimeter (Quantum Design PPMS).

## Acknowledgments

This work was supported by National Natural Science Foundation of China under contract No. U2032213. A portion of this work was supported by the High Magnetic Field Laboratory of Anhui Province.

## References

- [1] Mermin, N. D. & Wagner, H. Absence of Ferromagnetism or Antiferromagnetism in One- or Two-Dimensional Isotropic Heisenberg Models. *Phys. Rev. Lett.* **17**, 1133-1136 (1966).
- [2] Giamarchi, T. Theoretical framework for quasi-one dimensional systems. *Chem. Rev.* **104**, 5037–5056 (2004).
- [3] Kimura, S. Takeuchi, T. Okunishi, K. Hagiwara, M. He, Z. Kindo, K. Taniyama, T. & Itoh, M. Novel ordering of an S=1/2 quasi one-dimensional Ising-like antiferromagnet in magnetic field. *Phys. Rev. Lett.* **100**, 057202 (2008).
- [4] Klanjsek, M. Horvatic, M. Kramer, S. Mukhopadhyay, S. Mayaffre, H. Berthier, C. Canevet, E. Grenier, B. Lejay, P. & Orignac, E. Giant magnetic field dependence of the coupling between spin chains in BaCo<sub>2</sub>V<sub>2</sub>O<sub>8</sub>. *Phys. Rev. B* **92**, 060408 (2015).
- [5] Faure, Q. Takayoshi, S. Petit, S. Simonet, V. Raymond, S. Regnault, L. P. Boehm, M. White, J. S. Månsson, M. Rüegg, C. Lejay, P. Canals, B. Lorenz, T. Furuya, S. C. Giamarchi, T. & Grenier, B. Topological quantum phase transition in the Ising-like

- antiferromagnetic spin chain BaCo<sub>2</sub>V<sub>2</sub>O<sub>8</sub>. *Nat. Phys.* **14**, 716-722 (2018).
- [6] Pato-Doldán, B. Gómez-Aguirre, L. C. Hansen, A. P. Mira, J. Castro-García, S. Sánchez-Andújar, M. Señarís-Rodríguez, M. A. Zapf, V. S. & Singleton, J. Magnetic transitions and isotropic versus anisotropic magnetic behaviour of [CH<sub>3</sub>NH<sub>3</sub>][M(HCOO)<sub>3</sub>] M=Mn<sup>2+</sup>, Co<sup>2+</sup>, Ni<sup>2+</sup>, Cu<sup>2+</sup> metal-organic perovskites. *J. Mater. Chem. C* **4**, 11164-11172 (2016).
- [7] Li, W. Wang, Z. M. Deschler, F. Gao, S. Friend, R. H. & Cheetham, A. K. Chemically diverse and multifunctional hybrid organic-inorganic perovskites. *Nat. Rev. Mater.* **2**, 10669 (2017).
- [8] Bonner, J. C. & Fisher, M. E. Linear magnetic chains with anisotropic coupling. *Phys. Rev.* **135**, A640-A658 (1964).
- [9] Ma, L. Wang, Z. Hu, L. Qu, Z. Hao, N. & Pi, L. Magnetic field tuning of quantum spin excitations in a weakly coupled S=1/2 Heisenberg spin chain as seen from NMR. *Phys. Rev. B* **100**, 125126 (2019).
- [10] Johnston, D. C. Kremer, R. K. Troyer, M. Wang, X. & Canfield, P. C. Thermodynamics of spin S=1/2 antiferromagnetic uniform and alternating-exchange Heisenberg chains. *Phys. Rev. B* **61**, 9558-9606 (2000).
- [11] Belik, A. A. Uji, S. Terashima, T. & Takayama-Muromachi, E. Long-range magnetic ordering of quasi-one-dimensional S=1/2 Heisenberg antiferromagnet Sr<sub>2</sub>Cu(PO<sub>4</sub>)<sub>2</sub>. *J. Solid. State. Chem.* **178**, 3461-3463 (2005).
- [12] Drillon, M. Belaiche, M. Legoll, P. Aride, J. Boukhari, A. & Moqine, A. 1D ferrimagnetism in copper(II) trimetric chains: Specific heat and magnetic behavior of A<sub>3</sub>Cu<sub>3</sub>(PO<sub>4</sub>)<sub>4</sub> with A=Ca, Sr. *J. Magn. Magn. Mater.* **128**, 83-92 (1993).
- [13] He, Z. Z. Kyômen, T. & Itoh, M. BaCu<sub>2</sub>V<sub>2</sub>O<sub>8</sub>: Quasi-one-dimensional alternating chain compound with a large spin gap. *Phys. Rev. B* **69**, 220407(R) (2004).
- [14] Estes, W. E. Gavel, D. P. Hatfield, W. E. & Hodgson, D. J. Magnetic and structural characterization of dibromo- and dichlorobis(thiazole)copper(II). *Inorg. Chem.* **17**, 1415-1421 (1978).
- [15] Ma, Y. W. Lu, Y. H. Yi, J. B. Feng, Y. P. Heng, T. S. Liu, X. Gao, D. Q. Xue, D. S. Xue, J. M. Ouyang, J. Y. & Ding, J. Room temperature ferromagnetism in Teflon due to carbon dangling bonds. *Nat. Commun.* **3**, 727 (2012).
- [16] Lake, B. Tennant, D. A. Frost, C. D. & Nagler, S. E. Quantum criticality and universal scaling of a quantum antiferromagnet, *Nat. Mater.* **4**, 329-334 (2005).
- [17] Satija, S. K. Axe, J. D. Shirane, G. Yoshizawa, H. & Hirakawa, K. Neutron scattering study of spin waves in one-dimensional antiferromagnet KCuF<sub>3</sub>, *Phys. Rev. B* **21**, 2001-2007 (1980).
- [18] Hutchings, M. T. Samuelsen, E. J. Shirane, G. & Hirakawa, K. Neutron-Diffraction Determination of the Antiferromagnetic Structure of KCuF<sub>3</sub>, *Phys. Rev.* **188**, 919-923 (1969).
- [19] Kojima, K. M. Fudamoto, Y. Larkin, M. Luke, G. M. Merrin, J. Nachumi, B. Uemura, Y. J. Motoyama, N. Eisaki, H. Uchida, S. Yamada, K. Endoh, Y. Hosoya, S. Sternlieb, B. J. & Shirane, G. Reduction of Ordered Moment and Néel Temperature of Quasi-One-Dimensional Antiferromagnets Sr<sub>2</sub>CuO<sub>3</sub> and Ca<sub>2</sub>CuO<sub>3</sub>, *Phys. Rev. Lett.* **78**, 1787-1790 (1997).

- [20] Matsuda, M. Katsumata, K. Kojima, K. M. Larkin, M. Luke, G. M. Merrin, J. Nachumi, B. Uemura, Y. J. Eisaki, H. Motoyama, N. Uchida, S. & Shirane, G. Magnetic phase transition in the  $S=1/2$  zigzag-chain compound  $\text{SrCuO}_2$ , *Phys. Rev. B* **55**, R11953-R11956 (1997).
- [21] Zaliznyak, I. A. Broholm, C. Kibune, M. Nohara, M. & Takagi, H. Anisotropic Spin Freezing in the  $S=1/2$  Zigzag Chain Compound  $\text{SrCuO}_2$ , *Phys. Rev. Lett.* **83**, 5370-5373 (1999).
- [22] Zheludev, A. Kenzelmann, M. Raymond, S. Ressouche, E. Masuda, T. Kakurai, K. Maslov, S. Tsukada, I. Uchinokura, K. & Wildes, A. Energy Separation of Single-Particle and Continuum States in an  $S=1/2$  Weakly Coupled Chains Antiferromagnet, *Phys. Rev. Lett.* **85**, 4799-4802 (2000).
- [23] Tsukada, I. Sasago, Y. Uchinokura, K. Zheludev, A. Maslov, S. Shirane, G. Kakurai, K. & Ressouche, E.  $\text{BaCu}_2\text{Si}_2\text{O}_7$ : A quasi-one-dimensional  $S=1/2$  antiferromagnetic chain system, *Phys. Rev. B* **60**, 6601-6607 (1999).
- [24] Zheludev, A. Kakurai, K. Masuda, T. Uchinokura, K. & Nakajima, K. Dominance of the Excitation Continuum in the Longitudinal Spectrum of Weakly Coupled Heisenberg  $S=1/2$  Chains, *Phys. Rev. Lett.* **89**, 197205 (2002).
- [25] Nath, R. Mahajan, A. V. Buttgen, N. Kegler, C. Loidl, A. & Bobroff, J. Study of one-dimensional nature of  $S=1/2$   $(\text{Sr,Ba})_2\text{Cu}(\text{PO}_4)_2$  and  $\text{BaCuP}_2\text{O}_7$  via  $^{31}\text{P}$  NMR, *Phys. Rev. B* **71**, 174436 (2005).
- [26] Johannes, M. D. Richter, J. Drechsler, S.-L. & Rosner, H.  $\text{Sr}_2\text{Cu}(\text{PO}_4)_2$ : A real material realization of the one-dimensional nearest neighbor Heisenberg chain, *Phys. Rev. B* **74**, 174435 (2006).

## Contributions

Z.Q. supervised the project. Z. W. and L. H. grew the single crystal. Z. W., L. H., L. S. L., Y. Y. H. and J. T. X. carried out the experiments. Z. W., N. H. and Z. Q. analyzed the data and wrote the paper. All the authors discussed the results and commented on the manuscript.

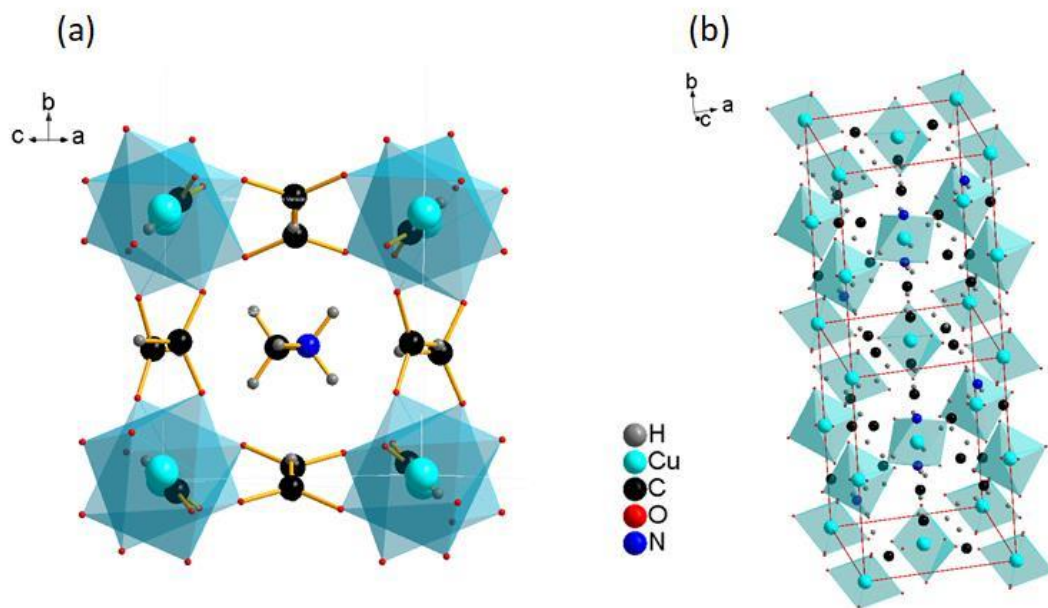


Fig. 1. Top view (a) and side view (b) of the perovskite-like structure of  $[\text{CH}_3\text{NH}_3][\text{Cu}(\text{HCOO})_3]$ .  $\text{CH}_3\text{NH}_3^+$  occupied the pseudo cubic cavity formed by  $\text{Cu}^{2+}$  and  $\text{HCOO}^-$ .  $\text{Cu}^{2+}$  ions in the endpoints of chains constitute a 2D square lattice.

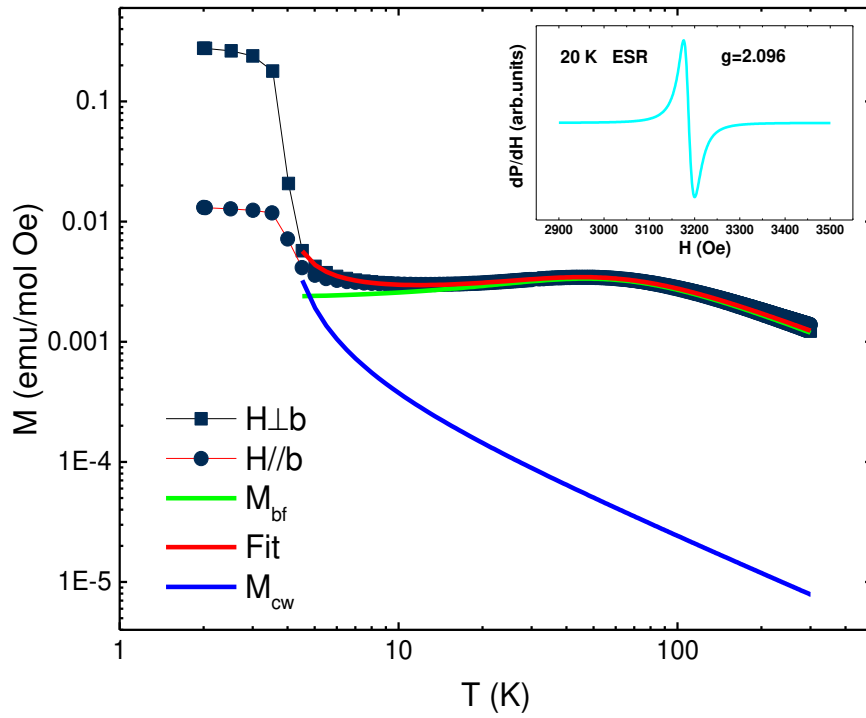


Fig. 2. Temperature dependence of the static magnetic susceptibility  $\chi = M/H$  measured at 200 Oe for  $H$  parallel and vertical to  $b$  axis above 4 K. Static magnetic susceptibility  $\chi = M/H$  of MACuF, at  $B=200$  Oe. The red line represents the fit by Eq. (2). The green line is contribution of  $\chi_{\text{chain}}$ . The blue line is Curie-Weiss paramagnetic susceptibility. The inset shows the ESR spectra at 20 K.

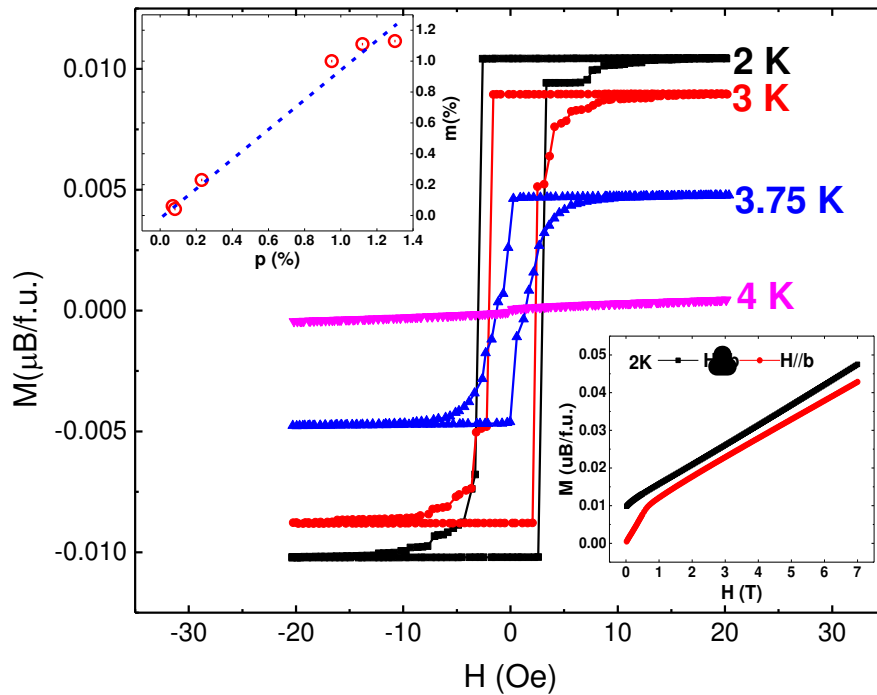


Fig.3 Magnetization ( $M$ ) versus applied field ( $H$ ) at four different temperatures for  $H \perp b$ . Top inset: paramagnetic term ratio ( $p$ ) of six different samples obtained by fitting Eq.(2) versus the ratio of the ferromagnetic saturation magnetic moment to that of  $\text{Cu}^{2+}$  ( $m = M_S / M_{\text{Cu}^{2+}}$ ). The dotted line represents the linear fitting to the data. Bottom inset:  $M$ - $H$  curve at 2K for  $H \perp b$  and  $H // b$  directions.

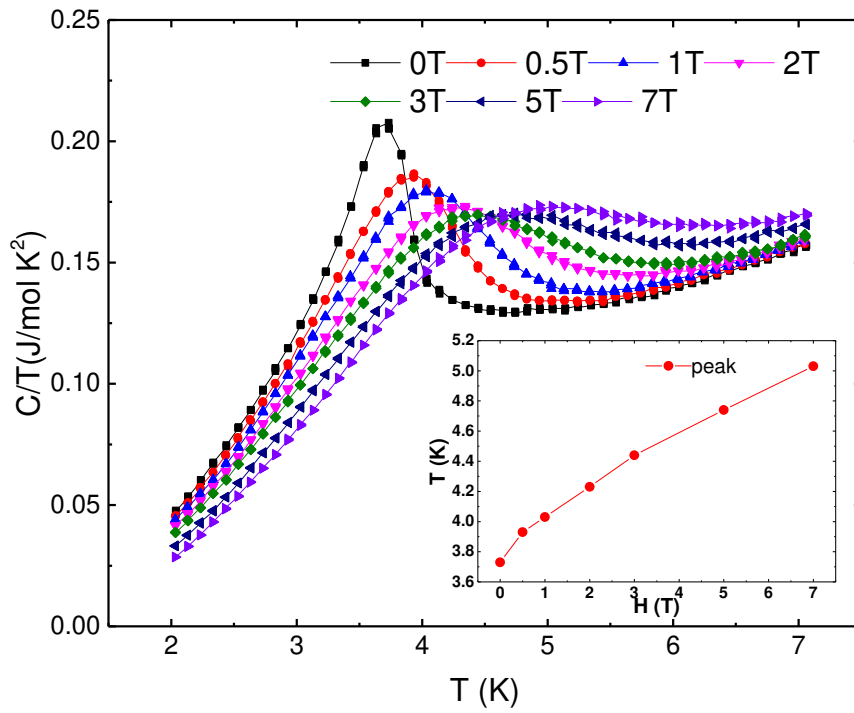
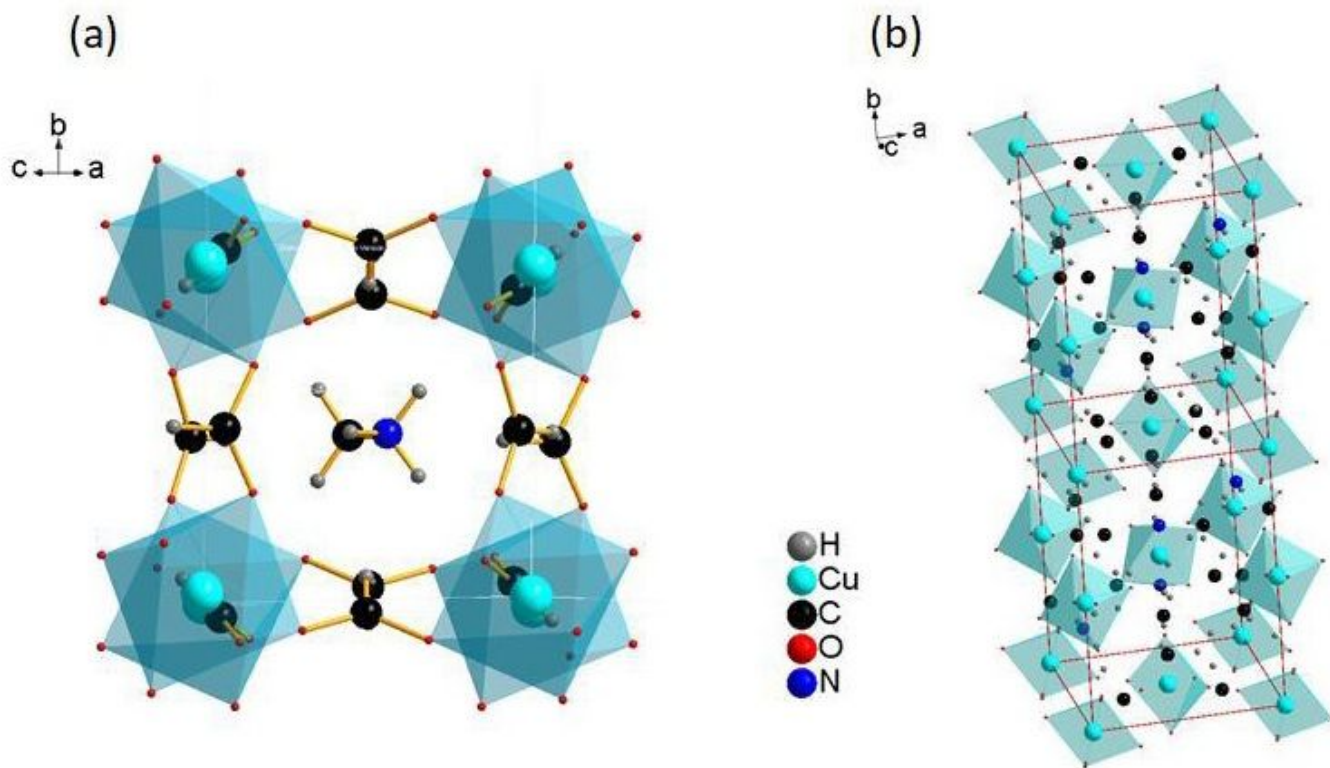


Fig. 4 Low temperature specific heat data measured in different fields for  $H//b$  direction. The inset shows the evolution of the specific heat peak with the applied magnetic field.

# Figures



**Figure 1**

Top view (a) and side view (b) of the perovskite like structure of  $[\text{CH}_3\text{NH}_3][\text{Cu}(\text{HCOO})_3]$ .  $\text{CH}_3\text{NH}_3^+$  occupied the pseudo cubic cavity formed by  $\text{Cu}^{2+}$  and  $\text{HCOO}^-$ .  $\text{Cu}^{2+}$  ions in the endpoints of chains constitute a 2D square lattice.

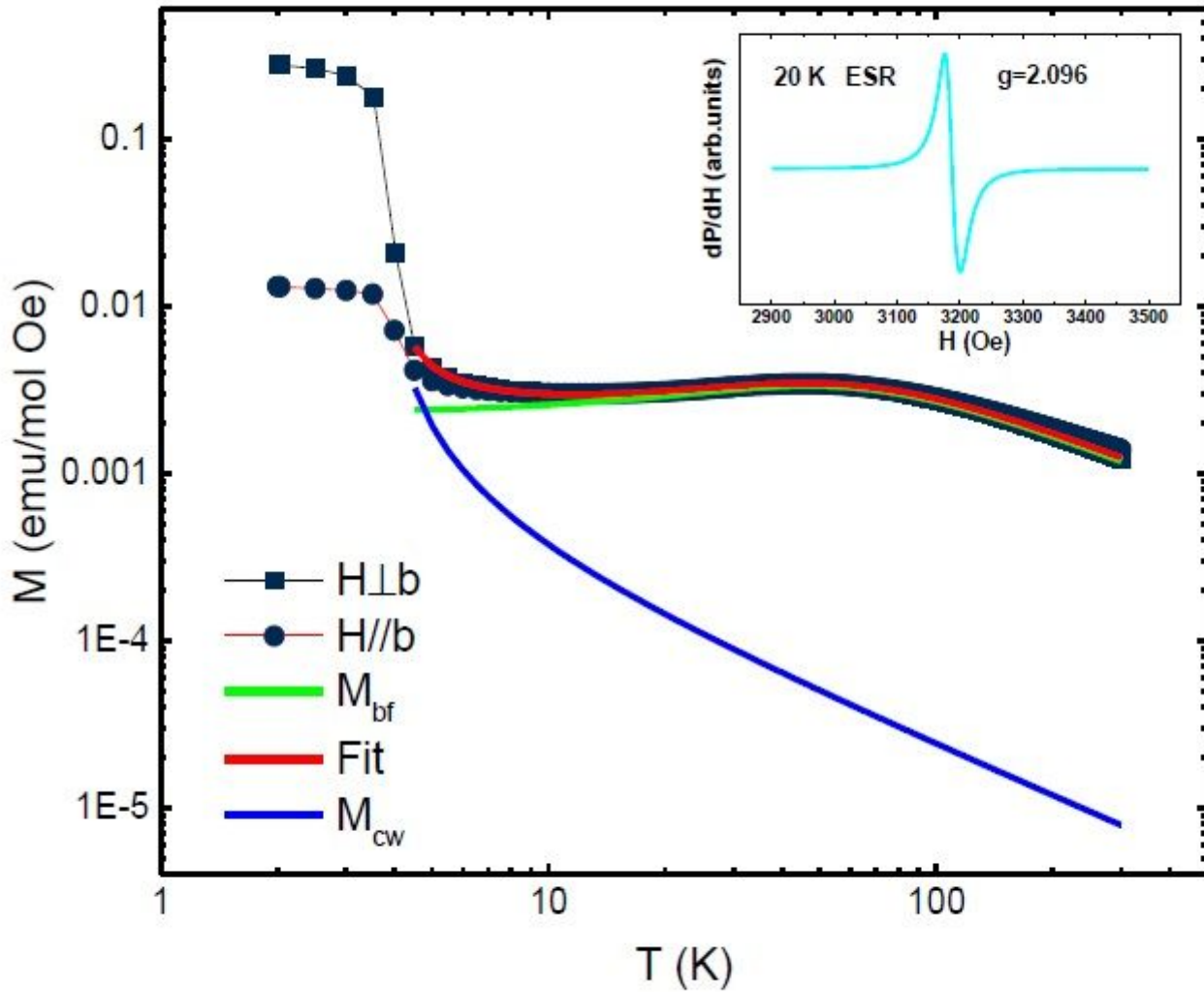


**Figure 2**

Temperature dependence of the static magnetic susceptibility  $\chi = M/H$  measured at 200 Oe for H parallel and vertical to b axis above 4 K. Static magnetic susceptibility  $\chi = M/H$  of MACuF, at B=200 Oe. The red line represents the fit by Eq. (2). The green line is contribution of  $\chi_{chain}$ . The blue line is Curie-Weiss paramagnetic susceptibility. The inset shows the ESR spectra at 20 K.

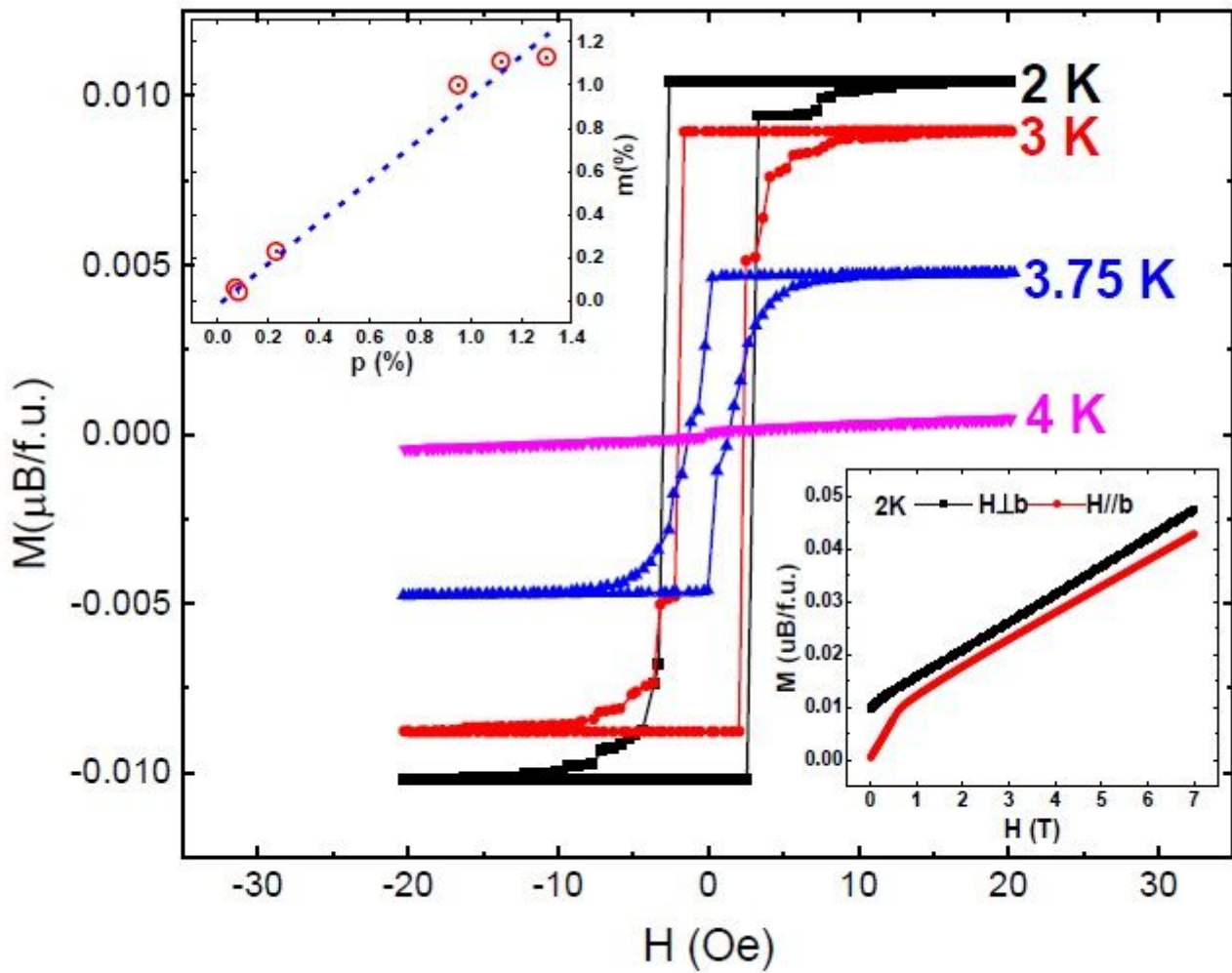


**Figure 3**

Magnetization ( $M$ ) versus applied field ( $H$ ) at four different temperatures for  $H \parallel b$ . Top inset: paramagnetic term ratio ( $p$ ) of six different samples obtained by fitting Eq.(2) versus the ratio of the ferromagnetic saturation magnetic moment to that of  $\text{Cu}^{2+}$  ( $m = \mu_B / \mu_B \text{Cu}^{2+}$ ). The dotted line represents the linear fitting to the data. Bottom inset:  $M$ - $H$  curve at 2K for  $H \parallel b$  and  $H \parallel a$  directions.

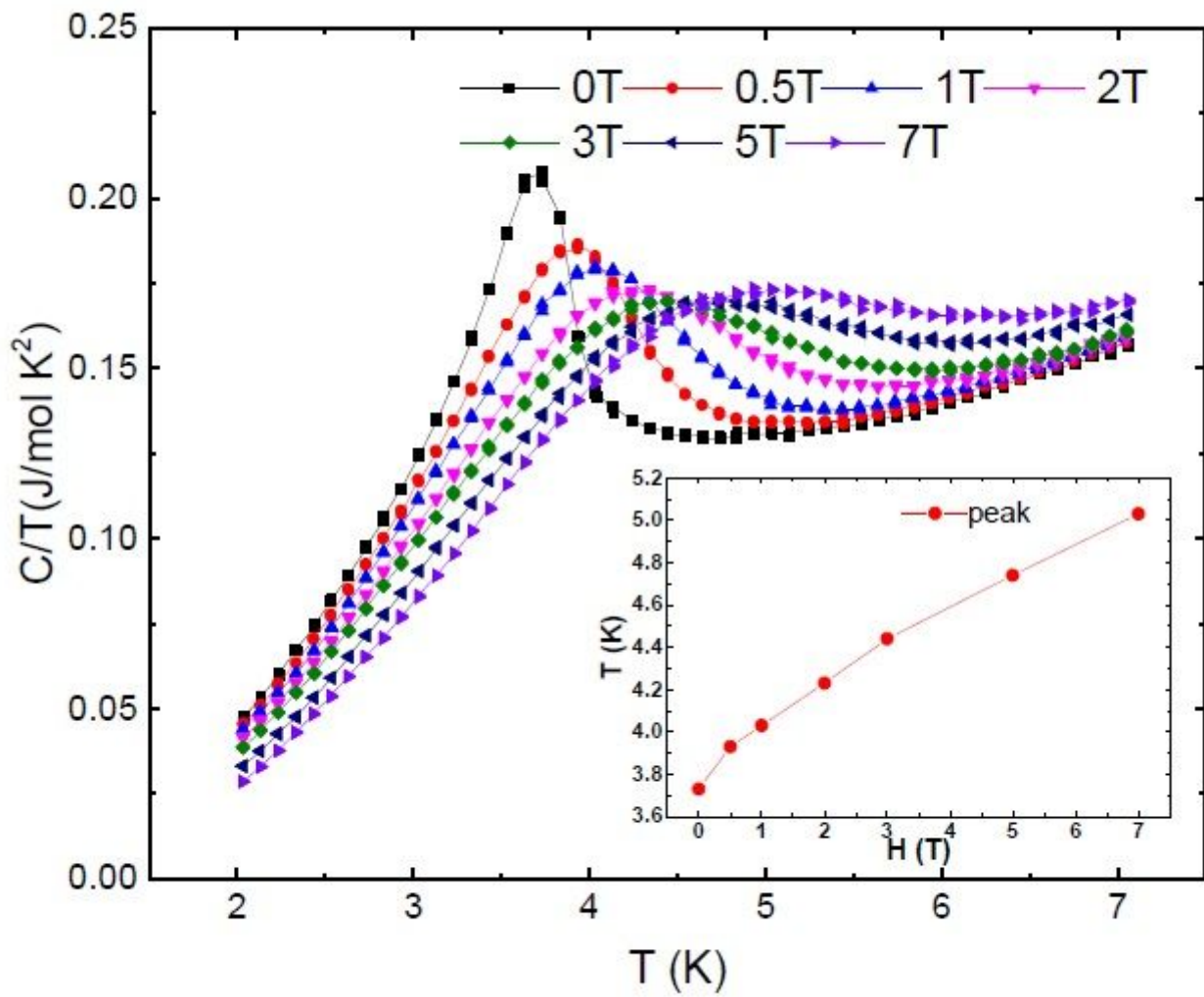


**Figure 4**

Low temperature specific heat data measured in different fields for  $H//b$  direction. The inset shows the evolution of the specific heat peak with the applied magnetic field.